PROCEEDINGS, 48th Workshop on Geothermal Reservoir Engineering
Stanford University, Stanford, California, February 6-8, 2023
SGP-TR-224

Thermal Hydraulics Evaluation of Fluid Flow Distribution in a Multi-Stage Stimulated Enhanced Geothermal System Wellbore at the Utah FORGE

Benjamin Willis[1,2] and Robert Podgorney[2]

[1]College of Engineering and Applied Science, University of Wyoming, Laramie, WY

[2]Advanced Scientific Computing, Idaho National Laboratory, Idaho Falls, ID

bwillis2@uwyo.edu robert.podgorney@inl.gov

Keywords: EGS, Utah FORGE, well hydraulics

ABSTRACT

Utilizing each flow path as evenly as possible is crucial to operate an Enhanced Geothermal System (EGS) at its highest potential and achieve efficient heat recovery. However, accomplishing this task can be complicated, as the fluid will always choose the path of least resistance, which can lead to uneven flow distribution. This study utilizes an analytical model and computational fluid dynamics (CFD) approaches to examine the sensitivity of an EGS to parameters such as perforations, fracture permeability, and flowrate in order to achieve as even fluid distribution as possible.

Operation of an EGS site will require an estimate of the pressure drop across the EGS in order to specify pumps and fluid handling equipment. Therefore, this study focused on pressure drop across the EGS and flow distribution percentage across each fracture zone. These two variables are plotted with varying input parameters such as number of perforations, excluding exit perforations, varying inlet flowrates, and varying fracture zone diameter throughout this paper.

1. INTRODUCTION

Previous analysis of flow through a well-fracture system representing the Utah FORGE site utilized an analytical model (Asai et al., 2022) consisting of a resistor system (Figure 1) that takes flow resistance into account for each EGS component (pipes, perforations, fractures) and estimates flow distribution across each fracture zone as well as pressure drop across the EGS. While fast and robust, this method has the drawback of not taking gravity, temperature, or fluid density/viscosity variations into account. Previous analysis by Asai et al. (2022) focused on generic EGS configurations containing 10 stimulated zones. For this analysis, the analytical model was configured to represent the Utah FORGE reservoir after the initial stimulation activities that took place in April 2022.

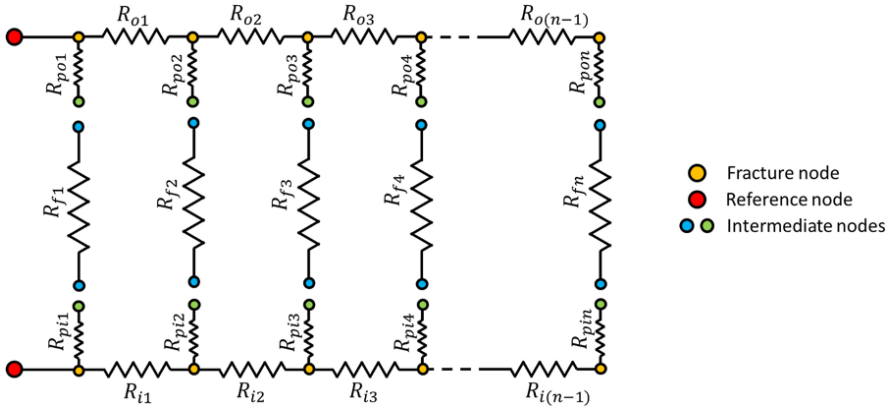

Figure 1: Analytical model resistor system.

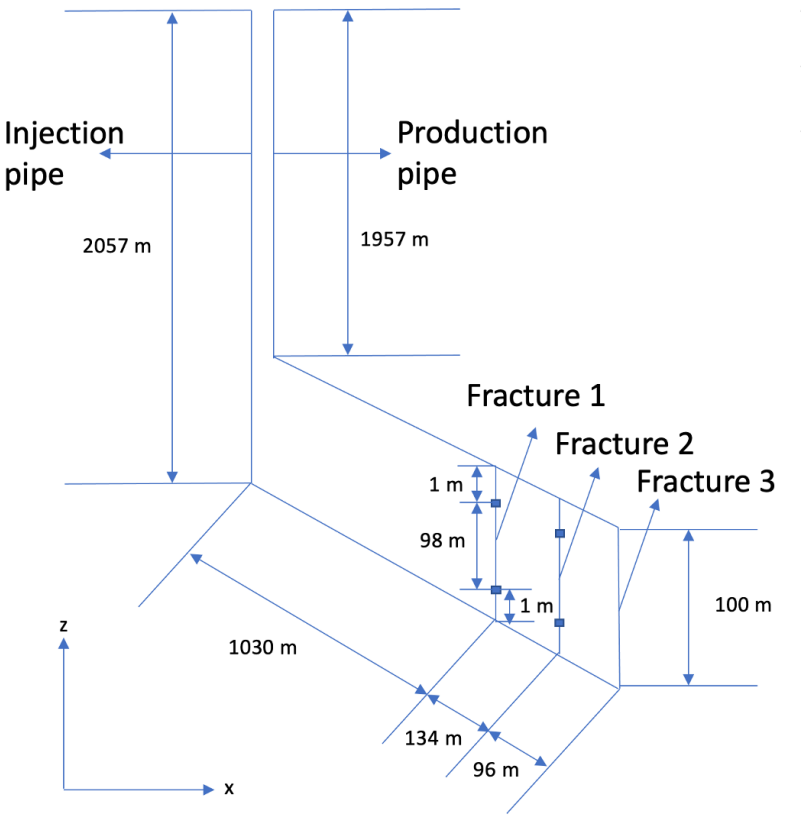

Figure 2: Thermal hydraulics model setup.

A thermal hydraulic model CFD model within the FALCON code (Podgorney et al., 2021; Lindsay et al., 2022) was also constructed utilizing the geometry of the Utah FORGE EGS site consisting of three fracture zones (see Figure 2, a second scenario with only two fracture zones was also evaluated), the full equation of state for water, well casing sizes, etc. The CFD simulations directly represented the inlet and exit perforations leading to the first two fracture zones closer to the heel of the well (Fracture 1 and Fracture 2). The third fracture zone closest to the toe of the well (Fracture 3) was designed to be an open hole with no perforations leading to the fracture zone. Perforations were turned on and off through setting the perforation flow channel diameters to the respective fracture zone diameter.

1.1 Conceptual Setup

Figure 3 below presents a conceptual schematic of the well-perforation-fracture zone. One of the key topics investigated as part of this study is the relationship between the number of effective perforations—that being the number of perforations that are in direct communication with fractures in the surrounding reservoir—and the potential impacts the pressure drop through the perforations can have on the distribution of flow exiting the injection well and entering the fractured reservoir. Well completion of the production well can also impact the flow distribution through the reservoir and additional pressure drop is expected for flow to enter a well through perforations.

For the analysis presentation that follows, permeability through the simulated fracture zones is uniform, i.e., potential reservoir heterogeneity is not evaluated and unless stated otherwise, 10 effective perforations (of 3/8” diameter) were simulated between the well and the reservoir.

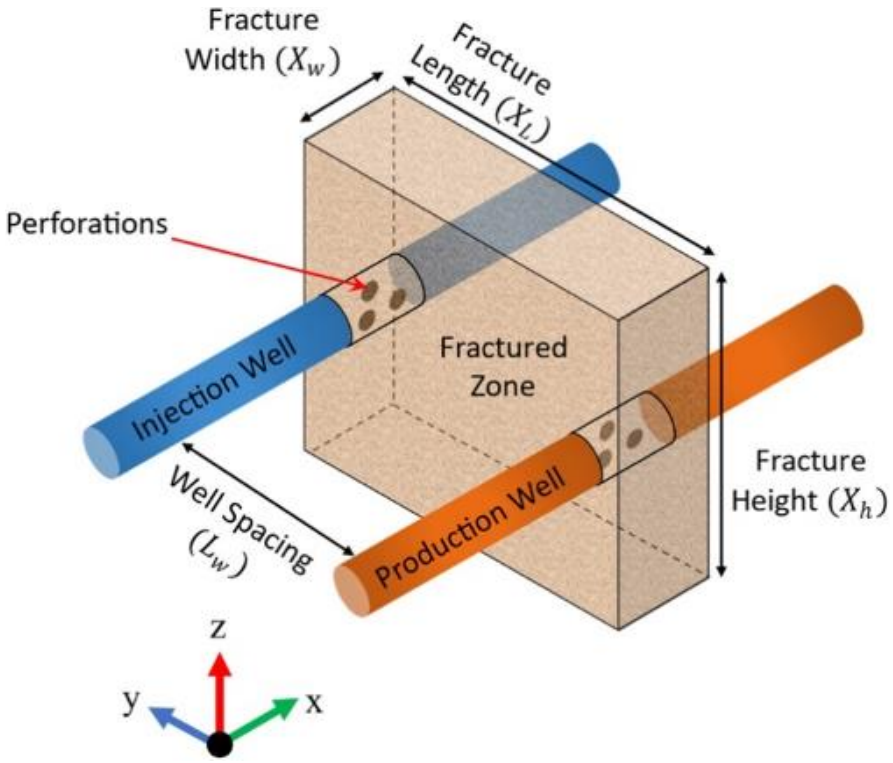

Figure 3: Conceptual schematic of the injection-production well pair, fracture zone, and perforations in the well casing (from Asai, et al., 2022).

1.2 Previous Analysis

Asai et al. (2022) performed a sensitivity study for flow distribution for EGS reservoirs with fully cased wells created with a plug-and-perf methodology. Asai's analysis focused on examining well doublet orientation configurations, perforation size, flow rates, and fracture zone permeability for well systems with 10 fracture zones. An example of the results as shown in Figure 4, which presents the sensitivity of flow distribution with perforation size. Asai et al. (2022) results showed that the parallel well EGS performed the poorest of all. The improvement in the flow distribution solely relies on creating a limited entry scenario (i.e., smaller diameter perforations near the heel of the injection well) at the fracture wellbore interface through smaller-diameter perforations, leading to increased pumping costs.

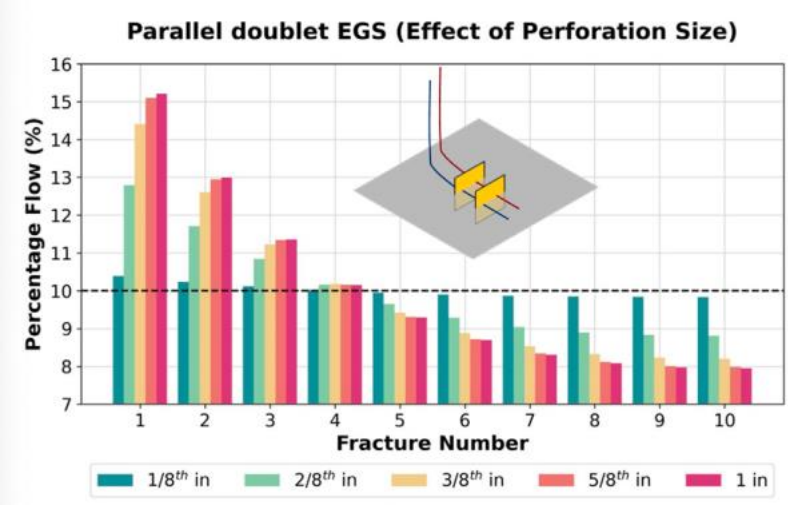

Figure 4: Sensitivity of flow distribution with perforation size (from Asai, et al., 2022).

Due to operational considerations and management decisions, it has been decided that the Utah FORGE will use a parallel well doublet design. This analysis was carried out to study and better inform design decisions related to the initial well design and completion for well 16B at the Utah FORGE site. Several scenarios were evaluated using both the analytical model developed by Asai et al. (2022) and a CFD approach.

For all cases evaluated in this effort, design of the simulations followed the planned or envisioned design for Utah FORGE. Well separation was set to 100m, with the to be drilled production well (16B) placed directly above and parallel to Well 16A.

2. SIMULATION PROCEDURE

The well pipe geometry was designed starting at ground level and immediately being affected by temperature and pressure gradients that vary with elevation. A cylindrical shell heat structure was set up for each pipe and fracture flow channel with a radius of 50 m. The heat structure associated with the pipes was designed with a section of the structure being dedicated to the pipe wall and the cement between the rock and pipe wall (Figure 6). The heat structure associated with the fractures was designed with no pipe wall or cement between the flow channel and the rock (Figure 6). The temperature and pressure initial and boundary conditions of the pipe geometry and heat structures were set with a linear interpolation varying with elevation, starting at 255°C at a depth of 0 m (ground level) and 196°C at a depth of -2800 m. The pressure was varied from 101.325 kPa at a depth of 0 m and 25.1865 MPa at a depth of -2666 m. The fluid properties utilized were initially stiffened gas fluid properties that had been approximated to water, with the IAPWS95 equation of state utilized for simulations competed later in the analysis.

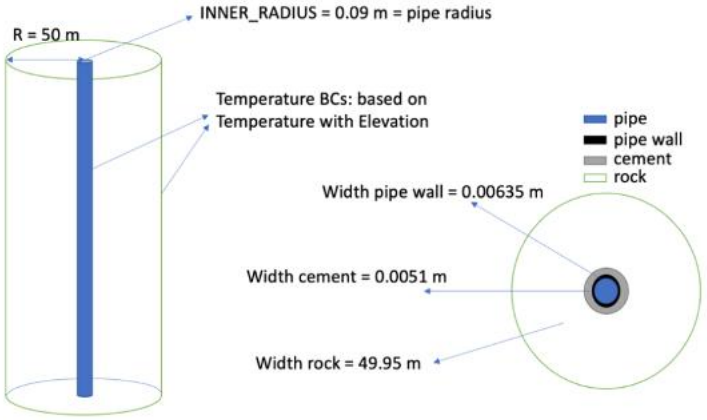

Figure 5: Cylindrical shell heat structure for pipe flow channels.

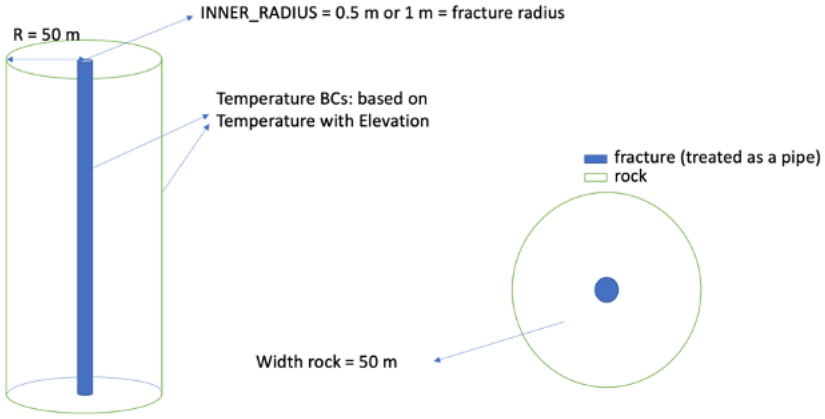

Figure 6: Cylindrical shell heat structure for fracture flow channels.

After the simulation configuration was set, postprocessors in the simulation code were set to report the pressure drop across each simulated fracture and across the EGS. Postprocessors were set up to monitor the mass flow rate going into each fracture as well as the temperature at the inlet and outlet of each fracture zone.

Fracture zone permeability, represented as pipes of various diameters, was approximated using Darcy's Law. The pressure drop across each fracture is used as well as the mass flowrate going into each fracture and the density and dynamic viscosity at the inlet and outlet of each fracture. Fracture permeability based on the density and dynamic viscosity was calculated and compared in the plots below.

The fracture diameter (represented as pipes) was varied using values of 0.5 m, 1 m, and 2 m. The mass flow rate was varied from 2 kg/s, 5 kg/s, and 10 kg/s. The CFD model results are shown for all three flowrate cases and only the 2 m fracture diameter case, as this fracture diameter may likely resemble conditions at the Utah FORGE site.

3. RESULTS

3.1 Analytical Three-Fracture Model Results

The analytical model results below are shown for a parallel well design (see Asai, et al., 2022) and the relationship between activating and deactivating exit perforations, the number of injection well perforations per fracture zone, and flow rate. In these cases, the injection well is assumed to be fully cased with the number of effective perforations varied from 1 to 100 in order to examine how the number of perforations affected the EGS performance. Flowrates of 5 and 10 kg/s are presented in this paper as the results are illustrative of the general behavior and are realistic to the initial planned Utah FORGE site flowrates for three fracture zones.

Figures 7 and 8 show the flow distribution percentage and pressure drop for 5 and 10 kg/s flow rates, respectively. As one can see on Figure 7, zones increasing the flowrate decreases the flow uniformity through the EGS, with the fracture zones nearest the heel of the well getting the majority of the flow (~ 35%). The presence or absence of perforations in the production well seemingly do not have a large impact on performance. The overall pressure drop along the EGS reservoir (Figure 8) does show an impact from the number of production well perforations, but after ~30 effective perforations are included the results are similar to the non-perforated case.

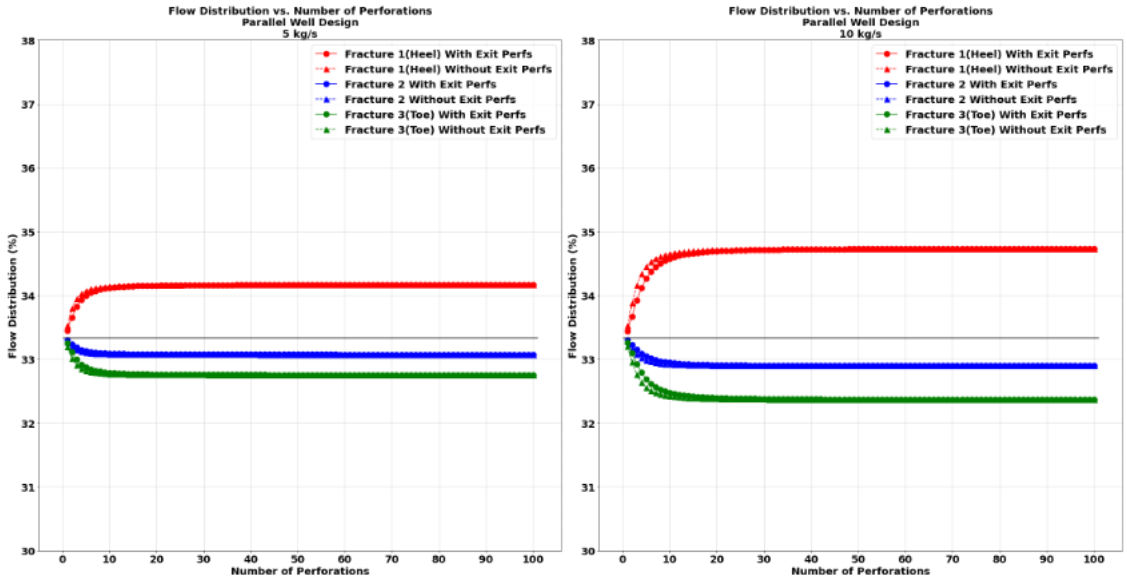

Figure 7: Flow distribution percentage from analytical model varying exit perforations.

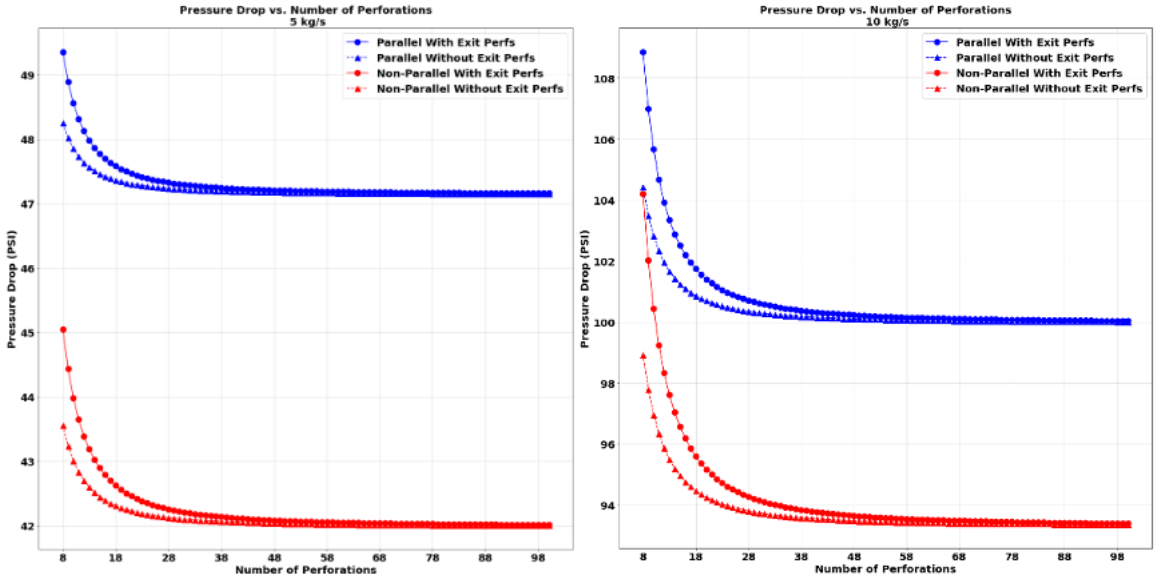

Figure 8: Pressure drop from analytical model varying exit perforations.

The next sensitivity that was tested with the analytical model was varying the fracture permeability from values of $1x10^{-12}$ and $1x10^{-14}$ m^2. The number of injection well perforations was varied from 1 to 60 to see how the number of perforations can affect the performance of the EGS reservoir. Figure 9 below shows the results for the 5 and 10 kg/s cases, and highlights that a low-permeability reservoir/fracture zones have a strong impact on flow distribution.

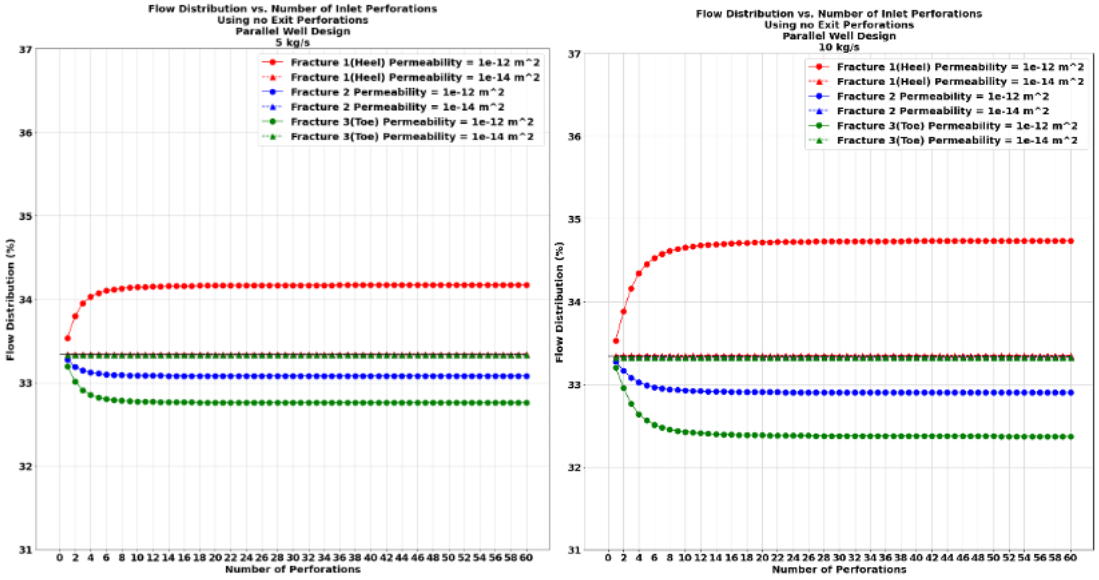

Figure 9: Flow distribution percentage from analytical model varying fracture permeability and injection well perforations

As stated earlier, the pressure drop across the EGS decreased asymptotically with the number of effective perforations. Figure 10 presents the pressure drop versus number of perforations for a single fracture zone ($1x10^{-12}$ m^2 permeability) for flow rates from 5 to 50 kg/s.

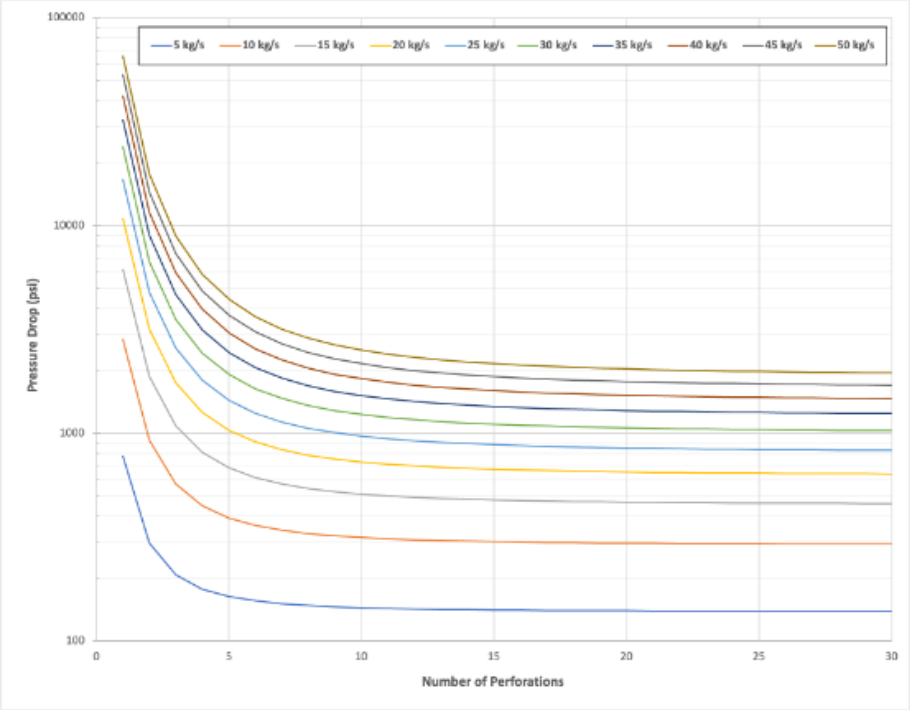

Figure 10: Pressure drop for a single fracture zone over various flow rates and number of perforations.

3.2 CFD Three-Fracture Model Results

The CFD modeling analysis presented here focuses on examining the flow distribution and pressure drop through the EGS reservoir. Three fracture zones are included, with the deepest fracture zone (toe of Well 16A) being treated as an open-hole completion (i.e., no perforation pressure drop) while the other two fracture zones are connected to the injection well through perforations in the well casing. The cases all used a uniform effective fracture permeability of $1x10^{-12}$ m^2 and a constant number of perforations (10) for zones that have them.

Figure 11 shows the flow distribution percentage for the three-fracture model for three flowrate cases 2 kg/s, 5 kg/s, and 10 kg/s, with the production well having a cased and perforated completion for fractures 1 and 2. Figure 12 shows the predicted flow distribution percentage through the EGS for the three-fracture model for the flowrate case of 5 kg/s with the production well having an open-hole completion (i.e., no perforation pressure drop associated with the production well). It is clear that from a thermal-hydraulics perspective, the differences in completion and effectiveness of the perforations can play a very important role in the effectiveness and sustainability of an EGS reservoir. The lack of a perforation pressure drop in the open-hole section of Well 16A is predicted to cause preferential flow through that zone of the well, for the lowest flow rete simulated (2 kg/s) ~ 92% of the fluid is predicted to flow through the open-hole section. For the highest flow rate simulated (10 kg/s) ~85% of the flow is predicted to flow through the open hole section. Removing the production well perforations, and treating Well 16B as having an open hole completion slightly changed these results (see Figure 12).

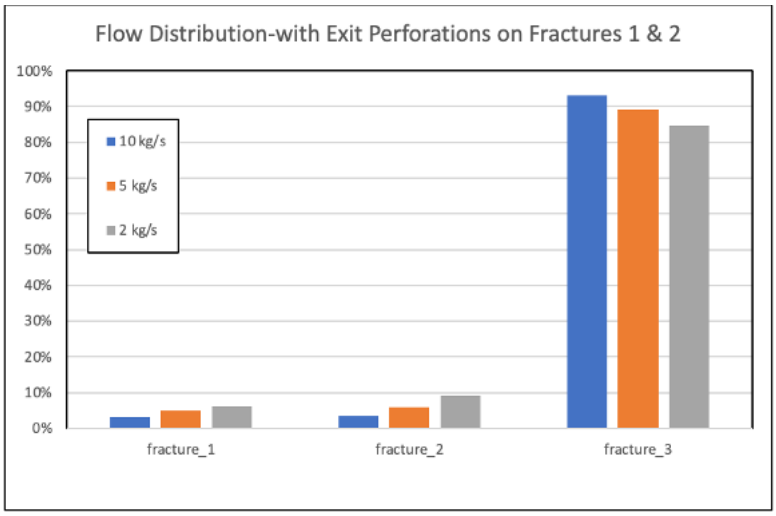

Figure 11: Flow distribution percentage for flow rates of 2, 5, and 10 kg/s with perforated production well.

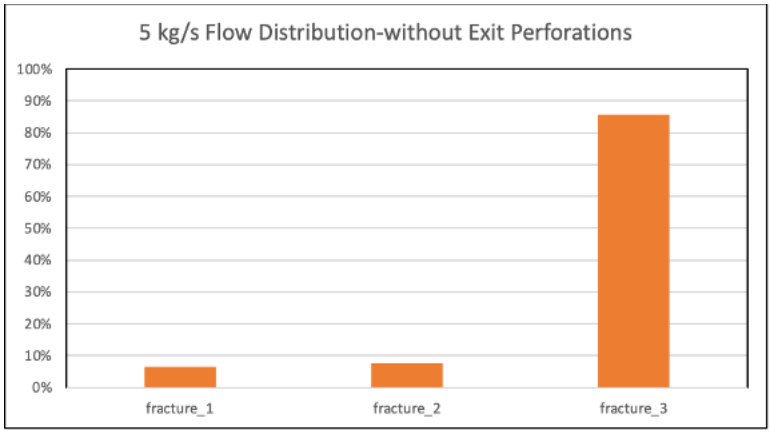

Figure 12: Flow distribution percentage for flow rate of 5 kg/s with no exit perforations (open-hole completion).

Figure 13 presents the pressure along the length of the injection pipe for the three-fracture model for three flowrate cases 2 kg/s, 5 kg/s, and 10 kg/s. Note that for all three flow rates, the predicted pressure at the top of the well head (bottom left corner of the data in Figure 13) is negative, indicating a thermal syphon condition at the top of the injection well. If this phenomenon proves to be correct it could have serious implications for operation of the reservoir.

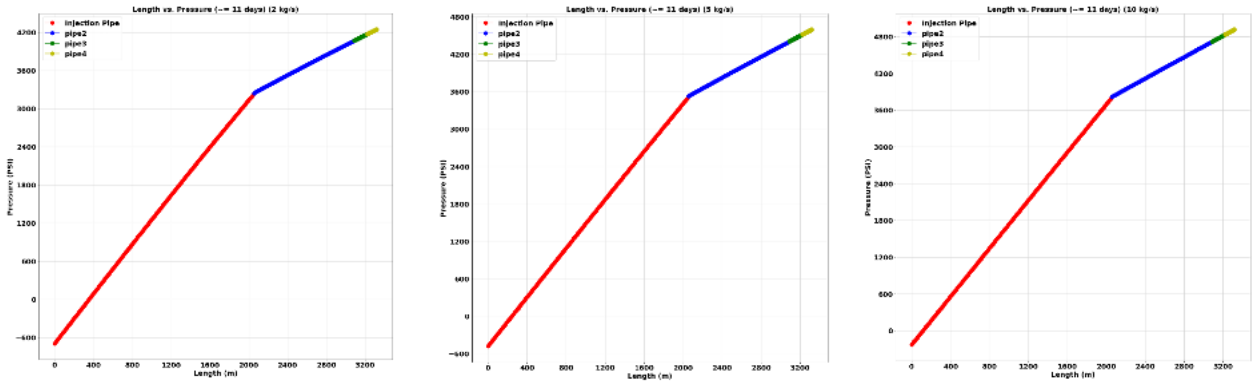

Figure 13: Injection well pressure distribution.

4. CONCLUSION

The analytical model results show that once approximately 30-40 perforations are reached, excluding exit perforations did not significantly alter the distribution. For the parallel well design, the lower permeability value of $1x10^{-14}$ m^2 yielded a nearly perfect flow distribution percentage across all fractures, however, this permeability value yielded unrealistically high pressure drops. Even though in the parallel case the flow distribution percentage was nearly perfect for the lower permeability value of $1x10^{-14}$ m^2, the pressure drop values suggest this permeability value is not feasible for a good EGS design.

The CFD model results for the three-fracture model show the flow distribution percentage with the open hole fracture at the toe getting approximately 90% of the flow and the other two fractures sharing the remaining 10% of the flow relatively equally. This is a reasonable estimate as to how the EGS would perform as the CFD model includes gravity, temperature, and pressure boundary conditions.

The calculated fracture permeability is less than ~$1x10^{-11}$ for most simulation cases which is useful for further applications of this model. Further applications of this model will incorporate real rock fractures in the current fracture zones that were simplified to pipes. This flow channel representing the fracture zones is a worse case scenario as the actual rock fractures will behave much differently and have a lower permeability value than the figures above. The pressure drop across the EGS that was estimated to be approximately 800 PSI, resulting a significant pressure drop across the EGS and potentially causing a large pumping cost.

This THM model will be utilized in the future with the fracture zones, that are currently being treated as pipes, being replaced with a realistic discrete fracture network to get a more accurate representation of the flow behavior in the EGS.

The source code for the analytical model can be accessed at: https://github.com/pranayasai/FlowDistribution

The data files and plots for the analytical model can be accessed at: https://github.com/BenjaminWillisINL/AnalyticalDataCSVs

The data files and plots for the THM model can be accessed at: https://github.com/BenjaminWillisINL/MOOSETHMModelCSVs

ACKNOWLEDGEMENTS

Funding for this work was provided by the U.S. DOE under grant DE-EE0007080 “Enhanced Geothermal System Concept Testing and Development at the Milford City, Utah FORGE Site.” We thank the many stakeholders who are supporting this project, including Smithfield, Utah School and Institutional Trust Lands Administration, and Beaver County as well as the Utah Governor’s Office of Energy Development.

REFERENCES

Asai, Pranay, et al. Analytical Model for Fluid Flow Distribution in an Enhanced Geothermal Systems (EGS). Renewable Energy, vol. 193, 18 May 2022, pp. 821-831., https://doi.org/10.1016/j.renene.2022.05.079.

Podgorney R., Finnila, A., Simmons, S., and McLennan, J. (2021). A Reference Thermal-Hydrologic-Mechanical Native State Model of the Utah FORGE Enhanced Geothermal Site. Energies, 14(16):4758. https://doi.org/10.3390/en14164758

Lindsay, A. D., Gaston, D. R., Permann, C. J., Miller, J. M., Andrš, D., Slaughter, A. E., Kong, F., Hansel, J., Carlsen, R. W., Icenhour, C., Harbour, L., Giudicelli, G. L., Stogner, R. H., German, P., Badger, J., Biswas, S., Chapuis, L., Green, C., Hales, J., … Wong, C. (2022). 2.0 - MOOSE: Enabling massively parallel multiphysics simulation. SoftwareX, 20, 101202. https://doi.org/https://doi.org/10.1016/j.softx.2022.101202